International Journal of Radiation Oncology biology • physics

www.redjournal.org

Clinical Investigation

Delineation of Neck Clinical Target Volume Specific to Nasopharyngeal Carcinoma Based on Lymph Node Distribution and the International Consensus Guidelines

Li Lin, MD,* Yao Lu, PhD,†,‡ Xiao-Ju Wang, MD,*,§ Hui Chen, BS,† Sha Yu, PhD,† Jiao Tian, MS,† Guan-Qun Zhou, MD,* Lu-Lu Zhang, MD,* Zhen-Yu Qi, PhD,* Jiang Hu, MS,* Jun Ma, MD,* and Ying Sun, PhD*

**Department of Radiation Oncology, Sun Yat-sen University Cancer Center, State Key Laboratory of Oncology in South China, Collaborative Innovation Center for Cancer Medicine, Guangzhou, People's Republic of China; †School of Data and Computer Science, Sun Yat-sen University, Guangzhou, People's Republic of China; ‡Guangdong Province Key Laboratory of Computational Science, Guangzhou, People's Republic of China; and §Department of Radiation Oncology, Hangzhou Cancer Center, Hangzhou, People's Republic of China*

Received Aug 19, 2017, and in revised form Oct 20, 2017. Accepted for publication Nov 1, 2017.

Summary

Neck LN distribution probability maps and curves for NPC were established based on 10,651 LNs from 956 patients. Relationships between the nodal distribution and international consensus guidelines for the delineation of neck LN levels were analyzed. Our findings demonstrate that most LN levels in the 2013 updated

Purpose: To establish the regional lymph node (LN) distribution probability map and draw the neck clinical target volume specific to nasopharyngeal carcinoma (NPC).

Methods and Materials: One thousand patients with pathologically proven NPC were enrolled from January 2010 to December 2011. The center point of the LNs with a minimal axial diameter of $\geq$4 mm was marked on a single treatment planning computed tomography scan. The neck LN levels I to X using the 2013 updated international consensus guidelines were also contoured. LN distribution probability maps and distribution curves were established. The relationships between the LN distribution and consensus guidelines were analyzed to propose modifications for clinical target volume boundaries specific to NPC.

Results: A total of 10,651 LNs from 959 patients were marked. Based on the distribution of LNs and consensus guidelines, most of the LN levels defined in the 2013 updated consensus guidelines were confirmed to be comprehensive and applicable for NPC.

Reprint requests to: Ying Sun, PhD, Department of Radiation Oncology, Sun Yat-sen University Cancer Center, State Key Laboratory of Oncology in South China, Collaborative Innovation Center of Cancer Medicine, 651 Dongfeng Rd East, Guangzhou 510060, People's Republic of China. Tel: (20) 8734-2253; E-mail: sunying@sysucc.org.cn

L.L., Y.L., and X.-J.W. contributed equally to the present study.

This study was supported by grants from the Sun Yat-sen University Clinical Research 5010 Program (grant 2012011), Health & Medical Collaborative Innovation Project of Guangzhou City, China (grant 201604020003), Special Support Program of Sun Yat-sen University Cancer Center (grant 16zxtzlc06), Innovation Team Development Plan of the Ministry of Education (grant IR_17R110), National Natural Science Foundation of China (No. 11401601), and Science and Technology Innovative Project of Guangdong Province, China (grant 2016B030337003).

Conflict of interest: none.

Supplementary material for this article can be found at www.redjournal.org.

Int J Radiation Oncol Biol Phys, Vol. 100, No. 4, pp. 891–902, 2018
0360-3016/$ - see front matter
https://doi.org/10.1016/j.ijrobp.2017.11.004

consensus guidelines are comprehensive and applicable for NPC. We have proposed a new level VIIc to include a medial group of retropharyngeal LNs, recommended moderately extended boundaries for levels Vb and VIIa, and suggested that boundaries for levels Ib, II, IV, and Vc might be reduced.

However, for level Vb, 13.3% of cases (11 of 83) had LNs beyond the posteromedial border. For level VIIa (retropharyngeal LN), 1.5% of cases (12 of 819) had LNs above the cranial boundary, and 5 cases had LNs that emerged in the medial group. Moreover, we confirmed that no LN had been detected in certain areas of levels Ib, II, IVa, and Vc. Accordingly, a new level VIIc was proposed to include the medial group of retropharyngeal LNs, moderately extended boundaries for levels Vb and VIIa were recommended, and reduced boundaries are possibly adaptable for levels Ib, II, IV, and Vc.

Conclusions: Most LN levels in the 2013 updated consensus guidelines are comprehensive and applicable for NPC. We have proposed a new level VIIc to include a medial group of retropharyngeal LNs, recommended moderate extended boundaries for levels Vb and VIIa, and suggested that the boundaries for levels Ib, II, IV, and Vc might be reduced.

Introduction

Early, widespread neck lymph node (LN) involvement is a well-recognized clinical feature of nasopharyngeal carcinoma (NPC) due to the vast submucosal avalvular lymph capillary network. Retrospective studies have shown that *ca.* 40% of LN-negative patients staged using palpation subsequently developed lymphadenectasis without elective neck irradiation (1). A meta-analysis reported that 85% of 2920 Chinese NPC patients staged using magnetic resonance imaging (MRI) had LN involvement at diagnosis (2). Therefore, elective neck irradiation was a standard recommendation for all patients in the conventional radiation therapy era, and continued in the intensity modulated radiation therapy (IMRT) era.

The highly conformal dose distribution of IMRT requires precise delineation of the gross tumor volume and clinical target volume (CTV). Precise knowledge of the normal neck LN anatomy and translation of the anatomic boundaries on computed tomography (CT) or MRI scans is crucial for delineation of the neck CTV during IMRT planning. CT-based international consensus guidelines for delineation of the neck CTV in LN-negative patients were proposed in 2003 based on the Robbins classification by major cooperative groups in Europe and North America (3). The guidelines were extended to include the LN-positive and postoperative neck in 2006 (4) and updated to include more comprehensive neck LN levels with more concise descriptions of anatomic boundaries in 2013 (5).

The guidelines facilitate uniform delineation of the neck CTV by radiation oncologists and enable institutions to share data. However, because these guidelines were primarily derived from patients with head and neck squamous cell cancer, whether they are optimal for NPC is unknown. With the aim of providing more suitable boundaries for neck CTV delineation in NPC, we established regional LN distribution probability maps using data from a large cohort of patients by marking the LNs on a single template CT scan and comparing the LN distribution for NPC with the 2013 updated consensus guidelines to draw neck CTV boundaries specific for NPC.

Methods and Materials

Patients

To establish the regional LN distribution probability map, 1000 patients with pathologically proven, nondisseminated NPC diagnosed from January 2010 to December 2011 were enrolled. The inclusion criteria for eligible patients were: (*1*) age $\geq$18 years; (*2*) baseline MRI scans of the nasopharynx and neck, with images stored in our institutional picture archiving and communication system; and (*3*) completed radical IMRT. We excluded patients with: (*1*) a history of head and neck surgery; (*2*) obvious artifacts on MRI that influenced the LN definitions; and/or (*3*) an insufficient MRI scanning scope to cover the nasopharynx and neck. The institutional review board approved the present study, and the requirement to obtain informed consent from the patients was waived. The authenticity of this article has been validated by uploading the key raw data onto the Research Data Deposit public platform (www.researchdata.org.cn), with the approval RDD number as RDDA2017000370.

Template CT scan

One patient's treatment planning CT scan with contrast was selected as the template for marking the exact position of the LNs. The selection criteria were: (*1*) T1N0 disease without obvious soft tissue masses; (*2*) no artifacts; (*3*) patient immobilized in the supine position with a "neutral" position using a head, neck, and shoulder thermoplastic mask; (*4*) without obvious bilateral asymmetry in the anatomic structures; (*5*) region from the head to 2 cm below the sternoclavicular joint included in the CT scan; and (*6*) enough fatty space to distinguish the anatomy.

The selected CT scan was captured in 3-mm slices from the head to 2 cm below the sternoclavicular joint (matrix size, 512 $\times$ 512; voxel resolution, 0.97 $\times$ 0.97 $\times$ 3.0 mm in the left−right, anteroposterior, and craniocaudal directions, respectively).

LN marking

Retropharyngeal LNs (LN_{RP}) and cervical LNs displaced on MRI scans with a minimal axial diameter (MID) of ≥4 mm were marked on the template CT scan slice-by-slice. Each eligible LN was manually marked at the equivalent location on the template CT scan with reference to the adjacent anatomic landmarks using the pretreatment MR image and original treatment planning CT scan. The referenced anatomic landmarks mainly included the main vessels, bones, muscles, and organs described in the 2013 updated international consensus guidelines. The MRI protocol and detailed standard operating procedure of LN marking has been described in Appendix E1 (available online at www.redjournal.org). Two independent operators participated; one marked the LNs (5 years of experience in radiation therapy for NPC) and another one independently reviewed the marked LNs (>15 years of experience in radiation therapy for NPC). Any disagreements were resolved by consensus. Any LN appearing in the medial retropharyngeal group was marked regardless of its size. Monaco, version 5.0 (Elekta AB, Stockholm, Sweden), was used for LN marking. Circles with a diameter of 3 mm (the smallest circle generated by Monaco) were used to mark the central point of each LN on all emerged slices. Visual examples of LN marking on the template CT scan are shown in Figure 1.

Cervical LNs marked on the template CT scan meeting the diagnostic criteria for LN metastases were defined as $LN_{\geq 10mm}$; LNs with a MID of 8 to 10 mm (11 mm for levels Ib and IIa) or 4 to 8 mm without any other positive criteria were designated as $LN_{8\text{-}10mm}$ and $LN_{4\text{-}8mm}$, respectively. The diagnostic criteria for positive cervical LNs were: (*1*) any cervical LN with a MID of ≥10 mm (levels Ib and IIa, ≥11 mm); (*2*) LNs of any size with central necrosis (defined as a focal area of high-signal intensity on T2-weighted images or a focal area of low-signal intensity on T1-weighted images with or without a contrast-enhanced rim); and (*3*) LNs of any size with extracapsular spread (defined as the presence of indistinct LN margins, irregular LN capsular enhancement, or infiltration into the adjacent fat or muscle).

The neck LN levels, including levels Ia, Ib, II, III, IVa, IVb, Va, Vb, Vc, VIa, VIb, VIIa, VIIb, VIII, IX, Xa, and Xb, were replicated on the template CT scan with reference to the 2013 updated consensus guidelines by 2 physicians in collaboration. To avoid potential bias in the LN level delineation, the marked LNs were blinded.

Data preparation

The template CT scan, marked LNs, and contoured neck LN levels were exported from Monaco in Digital Imaging and Communications in Medicine for radiation therapy format and converted into TXT format using in-house software developed in the Matrix Laboratory (MATLAB, 2015a; Mathworks, Natick, MA).

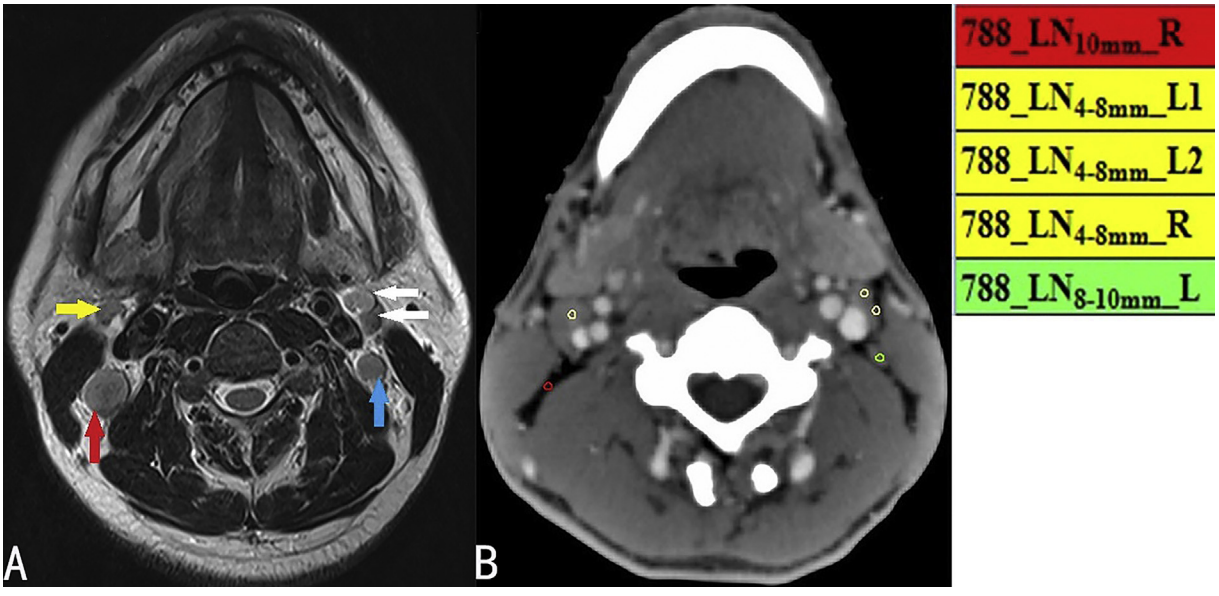

Fig. 1. Visual examples of lymph node (LN) marking on the template computed tomography (CT) scan. (A) Axial T2-weighted magnetic resonance images of a 35-year-old man showing 5 LNs in bilateral level II. The left level IIa nodes are 7 × 10 mm and 6 × 6 mm (white arrows), the left level IIb node is 9 × 10 mm (blue arrow), the right level IIa node is 6 × 9 mm (yellow arrow), and the right level IIb node is 14 × 15 mm (red arrow). (B) Template computed tomography scan at equivalent axial slice, 3-mm circles represent the center point of emerged LNs. The names of marked LNs consist of 3 parts connected using underscores, for example, in "788_$LN_{4\text{-}8mm}$_L1," 788 is the patient number in the cohort, $LN_{4\text{-}8mm}$ indicates the minimal axial diameter of this LN is 4 to 8 mm, and L1 indicates that this is the first LN defined in the left side of the neck.

Regional LN distribution characteristics

To study the regional LN distribution, the marked cervical LNs were organized in 3 patterns: (*1*) $LN_{\geq 10mm}$; (*2*) $LN_{\geq 8mm}$, combining $LN_{\geq 10mm}$ and $LN_{8\text{-}10mm}$; and (*3*) $LN_{\geq 4mm}$, combining $LN_{\geq 10mm}$, $LN_{8\text{-}10mm}$, and $LN_{4\text{-}8mm}$. Although the center point of each LN on all emerged slices was marked, only the center point of the median slice of each LN was used for analysis to minimize the mass and distortion effects of enlarged LNs. The LN distribution characteristics were summarized by patient and by LN. When summarized by patient, the incidence was defined as the ratio of the number of patients presenting with the LN at a certain level and the pattern and total patient number. When calculated by LN, the incidence was defined as the ratio of the number of LNs at a certain level and the pattern and total number of LNs in that pattern.

Regional LN distribution probability map and distribution curves

To generate the LN distribution probability map, first, the template CT scan was discretized to a 3-dimensional mesh with sphere grids (resolution, 6 mm). Next, the LN numbers within each grid were computed and translated into relative values, defined as the LN number within 1 grid divided by the maximum LN number within any of the grids. A color change was implemented to demonstrate the distinct relative values. Three heat maps were generated: $Map_{\geq 10mm}$, by LN_{RP} and $LN_{\geq 10mm}$; $Map_{\geq 8mm}$, by LN_{RP} and $LN_{\geq 8mm}$; and $Map_{\geq 4mm}$, by LN_{RP} and $LN_{\geq 4mm}$. The corresponding LN distribution curves ($DC_{\geq 10mm}$, $DC_{\geq 8mm}$, and $DC_{\geq 4mm}$) were generated to encircle all LNs in each pattern.

Relationship between distribution curves and 2013 updated consensus guideline LN levels

To draw the specific neck CTV for NPC using the 2013 updated consensus guidelines, the relationship between the $DC_{\geq 4mm}$ and consensus LN levels was analyzed by 2 radiation oncologists with >15 years of experience in radiation therapy for NPC. The LN levels were classified into 3 categories: (*1*) levels with no distribution curves generated; (*2*) levels with $DC_{\geq 4mm}$ completely included in the consensus LN levels; and (*3*) levels with $DC_{\geq 4mm}$ exceeding the consensus LN levels.

Results

Patient and regional LN distribution characteristics

The characteristics of the patients and regional LN distribution are summarized in Tables 1 and 2, respectively. Of the 1000 patients, 959 (95.9%) had LNs with a MID of ≥4 mm, of which 819 (85.4%) presented with LN_{RP}, 605 (63.1%) with $LN_{\geq 10mm}$, 353 (36.8%) with $LN_{8\text{-}10mm}$, and 945 (98.5%) with $LN_{4\text{-}8mm}$. A total of 10,651 LNs were marked: 1625 (15.3%) were LN_{RP} (level VIIa), 2693 (25.3%) were $LN_{\geq 10mm}$, 504 (4.7%) were $LN_{8\text{-}10mm}$, and 5829 (54.7%) were $LN_{4\text{-}8mm}$. In general, the incidence of $LN_{\geq 8mm}$ and $LN_{\geq 10mm}$ was similar for all LN levels. However, for $LN_{\geq 4mm}$, the incidence increased sharply, especially for level Ia, from 4 (0.08%) to 142 (1.3%), and level Ib, from 62 (1.3%) to 1084 (10.2%).

Of the 1625 LN_{RP}, 5 (0.3%) were located in the medial group. Only 2 LNs with a MID of 4 to 8 mm were found in level VIb, and no LN with a MID of ≥4 mm was found in level VIa. No $LN_{\geq 10mm}$ emerged in level Ia, VIa, or VIb.

Table 1 Characteristics of 1000 patients with nasopharyngeal carcinoma

Characteristic	Patients (n)
Sex	
Male	751 (75.1)
Female	249 (24.9)
Age (y)	
Median	45 (18-78)
>50	294 (29.4)
≤50	706 (70.6)
Histologic type	
Keratinizing squamous cell carcinoma	4 (0.4)
Nonkeratinizing carcinoma	996 (99.6)
T stage*	
T1	120 (12.0)
T2	134 (13.4)
T3	524 (52.4)
T4	222 (22.2)
N stage*	
N0	142 (14.2)
N1	559 (55.9)
N2	166 (16.6)
N3	133 (13.3)
Clinical stage*	
I	35 (3.5)
II	149 (14.9)
III	494 (49.4)
IV	322 (32.2)

Data in parentheses are percentages.

* Patients were restaged using the 8th edition of the American Joint Committee on Cancer/Union for International Cancer Control staging system.

Regional LN distribution probability maps

The probability maps ($Map_{\geq 10mm}$, $Map_{\geq 8mm}$, and $Map_{\geq 4mm}$) of the neck LN distribution are shown in Figure 2 through 5 typical transverse sections (the entire maps are shown in Figs. E1-E3; available online at www.redjournal.org). The color wash change from blue through yellow to red indicates the probability increase. From the probability maps, distinct LN distribution probabilities of

Table 2 Distribution of 10,651 lymph nodes in 959 patients

Level	Patients (n)			LNs (n)		
	$LN_{\geq 10mm}$	$LN_{\geq 8mm}$	$LN_{\geq 4mm}$	$LN_{\geq 10mm}$	$LN_{\geq 8mm}$	$LN_{\geq 4mm}$
Ia	0 (0)	4 (0.4)	115 (12.0)	0 (0)	4 (0.08)	142 (1.3)
Ib	24 (2.5)	51 (5.3)	548 (57.1)	30 (0.7)	62 (1.3)	1084 (10.2)
II	587 (61.2)	686 (71.5)	949 (99.0)	1945 (45.1)	2311 (47.9)	5446 (51.1)
III	170 (17.7)	194 (20.2)	509 (53.1)	448 (10.4)	508 (10.6)	1411 (13.2)
IVa	49 (5.1)	57 (5.9)	161 (16.8)	98 (2.3)	110 (2.3)	311 (2.9)
IVb	4 (0.4)	5 (0.5)	10 (1.0)	6 (0.1)	7 (0.1)	13 (0.1)
Va	64 (6.7)	76 (8.0)	235 (24.5)	89 (2.1)	104 (2.2)	365 (3.4)
Vb	23 (2.4)	30 (3.1)	83 (8.7)	46 (1.1)	57 (1.2)	157 (1.5)
Vc	2 (0.2)	2 (0.2)	6 (0.6)	2 (0.05)	2 (0.04)	7 (0.07)
VIa	0 (0)	0 (0)	0 (0)	0 (0)	0 (0)	0 (0)
VIb	0 (0)	0 (0)	2 (0.2)	0 (0)	0 (0)	2 (0.02)
VIIa (LN_{RP})	0 (0)	819 (85.4)	0 (0)	0 (0)	1625 (15.3)	0 (0)
VIIb	7 (0.7)	7 (0.7)	8 (0.8)	7 (0.2)	7 (0.1)	8 (0.08)
VIII	13 (1.4)	14 (1.5)	43 (4.5)	15 (0.3)	17 (0.4)	63 (0.6)
IX	1 (0.1)	1 (0.1)	2 (0.2)	1 (0.02)	1 (0.02)	2 (0.02)
Xa	1 (0.1)	1 (0.1)	1 (0.1)	1 (0.02)	1 (0.02)	1 (0.009)
Xb	3 (0.3)	4 (0.4)	11 (1.1)	3 (0.07)	4 (0.08)	11 (0.1)
Total	878 (91.6)	896 (93.4)	959 (100)	4316 (100)	4820 (100)	10,648 (100)

Abbreviations: $LN_{\geq 10mm}$ = cervical lymph nodes meeting the diagnostic criteria for lymph node metastases; $LN_{\geq 8mm}$ = cervical LNs with a minimal axial diameter of ≥8 mm or any size with central necrosis, a contrast-enhanced rim, or extracapsular spread; $LN_{\geq 4mm}$ = cervical LNs with a minimal axial diameter ≥4 mm or any size with central necrosis, a contrast-enhanced rim, or extracapsular spread; LN_{RP} = retropharyngeal lymph nodes (ie, level VIIa).

Data in parentheses are percentages.

different levels can be observed, and the detailed location of the LNs in each level can be intuitively exhibited. For example, from level II to Level IV, the LNs emerging before the carotid sheath become fewer.

Regional LN distribution curves

Visual examples of the distribution curves ($DC_{\geq 10mm}$, $DC_{\geq 8mm}$, and $DC_{\geq 4mm}$) and the 2013 updated consensus guidelines LN levels are shown in Figure 3 through 8 transverse sections (Fig. E4 gives the entire distribution curves; available online at www.redjournal.org). The distribution curves for $DC_{\geq 10mm}$ and $DC_{\geq 8mm}$ were nearly the same. When combined with $LN_{4\text{-}8mm}$, the LNs became more profuse in levels Ia, Ib, IVa, IVb, Vb, and Vc, and the distribution curve became markedly extended.

According to the relationships between $DC_{\geq 4mm}$ and the consensus guideline LN levels, level VIa had no distribution curve generated; levels Ib, II, III, IVa, IVb, Va, Vc, VIb, VIIa, VIIb, VIII, IX, Xa had distribution curves completely encompassed by the consensus guideline LN levels; and levels Vb and VIIa had distribution curves exceeding the boundaries defined in the consensus guidelines. More specifically, for level Vb, 13.3% of cases (11 of 83) had LNs beyond the posteromedial border. For level VIIa, 1.5% of cases (12 of 819) had LNs above the upper border, and 5 cases (0.3%) had LNs located in the medial group. Moreover, we confirmed that no LN had been detected in certain areas of levels Ib, II, IVa, and Vc.

Potential modifications for neck CTV specific to NPC

According to the LN distribution maps and distribution curves, the neck LN levels defined in the 2013 updated consensus guidelines are comprehensive enough and the boundaries described are applicable for most levels in most directions for NPC. However, by comparing the LN distribution and consensus guidelines, we have proposed a new level, level VIIc, to include a medial group of retropharyngeal LNs. To draw CTV boundaries specific to NPC, moderately extended boundaries for levels Vb and VIIa are recommended. Also, we suggest that reduced boundaries could possibly be adapted for levels Ib, II, IV, and Vc. Nevertheless, all these modifications should be validated in prospective clinical trials. The modifications are illustrated in Figure 4.

1. Level VIIc: For LN_{RP}, the consensus guidelines consider only the lateral group. In the present study, 5 cases (0.3%) had LNs located in the medial group, which seems to be a part of the neck lymphatic drainage network of NPC. None of the 5 LNs were below the caudal edge of second cervical vertebrae (C2). To better guide the elective irradiation of the neck levels for NPC, we have proposed a new level, level VIIc, to include the medial group of retropharyngeal LNs. The proposed boundaries extend cranially from the skull base to the caudal edge of the C2 vertebrae caudally. This space is bounded anteriorly by the pharyngeal constrictor muscles, posteriorly by the longus capitis, laterally by the

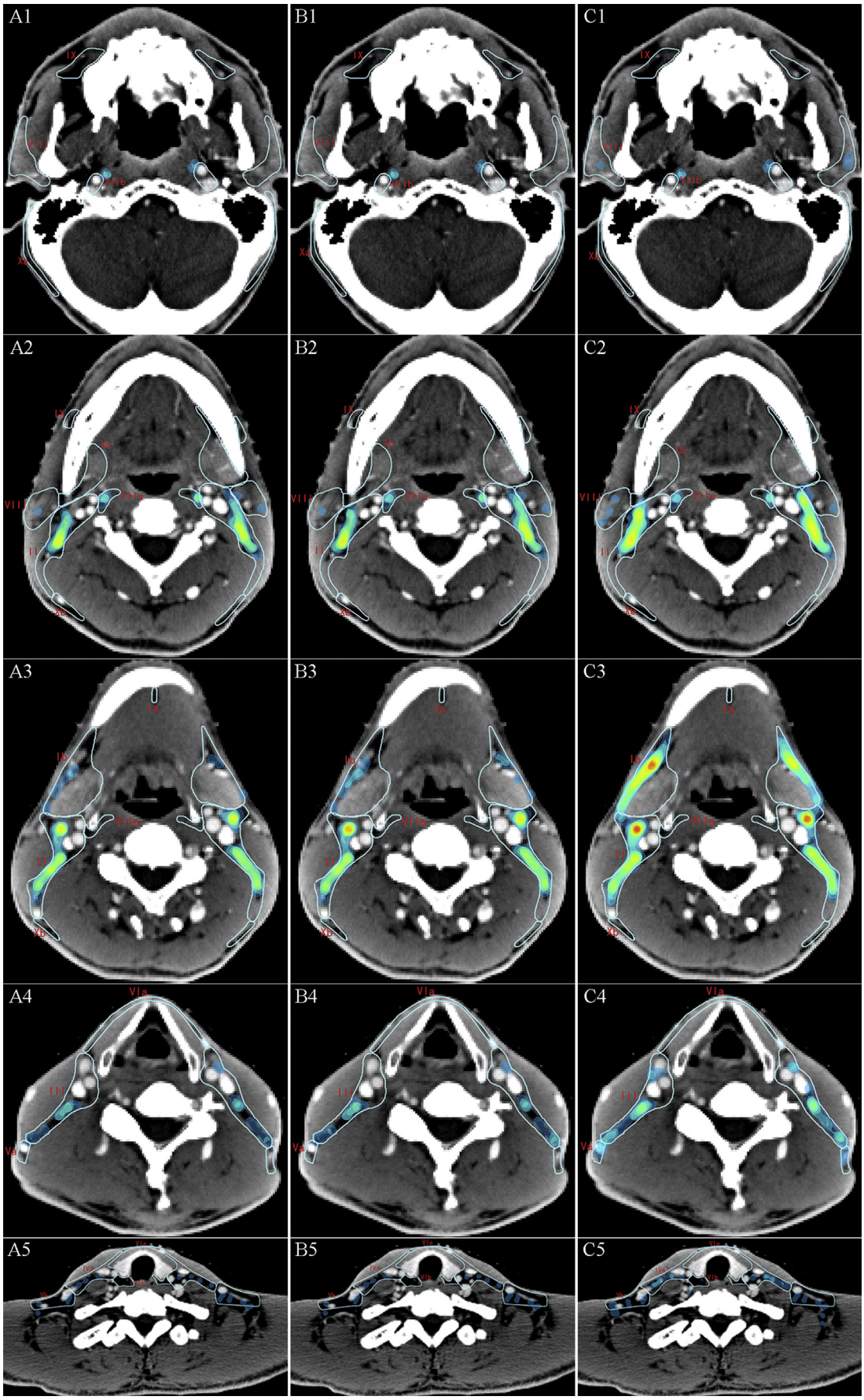
A1
B1
C1
A2
B2
C2
A3
B3
C3
A4
B4
C4
A5
B5
C5

medial boundary of level VIIa, and medially by the midline (Fig. 4A).

2. Level Vb: We confirmed that LNs emerged beyond the posteromedial border of level Vb in 13.3% of cases with level Vb LNs, scattering around the transverse blood vessels superficially to the anterior edge of the levator scapulae muscle. We recommend extending the posteromedial border of level Vb to the anterior edge of the levator scapulae muscle to include the transverse blood vessels (Fig. 4B).
3. Level VIIa: Because 12 cases with LNs exceeded the upper edge of the first cervical vertebrae (C1), we recommended extending the cranial border of level VIIa from the upper edge of the C1 vertebrae to the skull base (Fig. 4C).
4. Level Ib: The LNs in level Ib were all scattered laterally and anteriorly to the submandibular gland (SMG), and no LN was identified along the medial edge of SMG or within the gland parenchyma. Because the presence of intraglandular LNs has been disputed (6) and to eliminate xerostomia after radiation therapy (7), we suggest that the SMG could be spared when delineating the CTV for level Ib (Fig. 4D).
5. Level II: At the C1 and C2 vertebrae levels, the sternocleidomastoid and splenius capitis muscles are tightly integrated, and we confirmed that no LNs were detected in the gap between them. Accordingly, the gap between the sternocleidomastoid and splenius capitis muscle could be spared when delineating the CTV for level II where they are tightly integrated (Fig. 4E).
6. Level IVa: We confirmed that no LNs were identified in the gap between the sternocleidomastoid and infrahyoid ribbon muscles at level IVa. We suggest that the anterior border of level IVa might be modified from the anterior edge of the sternocleidomastoid to the posterior edge of the infrahyoid ribbon muscles (Fig. 4F).
7. Level Vc: We suggest that the anterior border of level Vc might be revised as omohyoid muscle to replace skin (Fig. 4G) as no LNs were identified in the gap between skin and omohyoid muscle.

Discussion

By marking 10,651 LNs in 959 patients, we first established regional LN distribution probability maps and distribution curves for NPC. The neck LN levels defined in the 2013 updated consensus guidelines were proved to be comprehensive enough and the boundaries described are applicable for most levels in most directions for NPC. Our objective was to address the boundaries of the neck LN levels specific to NPC using the neck LN distribution from a large patient cohort, rather than to generate recommendations for elective irradiation of the LN levels for NPC. In summary, we have proposed a new level, level VIIc, to include a medial group of retropharyngeal LNs, recommended moderately extended boundaries for levels Vb and VIIa, and suggested that the boundaries for levels Ib, II, IV, and Vc might be reduced.

Because all LNs were manually marked on a single template CT scan, the accuracy of LN marking is closely related to the reliability of the LN distribution, which determined our results. We believe the LN marking procedure was considerably accurate for 2 reasons. First, each LN was manually marked at the equivalent location of the template CT scan with reference to the adjacent anatomic landmarks using pretreatment MR images by an experienced radiation oncologist and independently checked by another more experienced radiation oncologist. Also, we always verified that the LNs marked at the specific location in the template CT scan were those observed on the original planning CT scan. Second, although the patient's head was slightly hyperextended in the template CT scan compared with the MR images owing to the use of the immobilization mask, the patients were all placed supine and in a "neutral" position. Because the anatomic landmarks adjacent to the LNs were used, the shifts of the anatomic landmarks and the LNs were always consistent when the position of the patients changed slightly.

Generally, the MID of 10 mm has been used as effective size criterion for metastatic LNs in clinical practice (8). van den Brekel et al (9) reported the diagnostic sensitivity of LN metastasis was only 41.7% per LN using a MID of 10 mm; using 8 and 6 mm increased the sensitivity to 54.2% and 69.4%, with a specificity of 96.8% and 91.9%, respectively. Using a MID of 10 mm, imaging will underestimate 12% to 50% of LN micrometastases (10-12). Another study found 16% of LNs defined on MR images using a MID of 4 to 9 mm were histologically metastatic compared with only 0.6% with an MID <4 mm (13). However, even with the use of modern imaging modalities, no reliable diagnostic tool is available to detect microscopic neck LN involvement in patients with clinically or

Fig. 2. Distribution probability maps for the lymph nodes (LNs) demonstrated through 5 typical transverse sections. (A1-A5) $Map_{\geq 10mm}$, established using retropharyngeal LNs (LN_{RP}) and $LN_{\geq 10mm}$; (B1-B5) $Map_{\geq 8mm}$, based on LN_{RP} and $LN_{\geq 8mm}$ ($LN_{\geq 10mm}$ plus $LN_{8\text{-}10mm}$); and (C1-C5) $Map_{\geq 4mm}$, based on LN_{RP} and $LN_{\geq 4mm}$ ($LN_{\geq 10mm}$ plus $LN_{8\text{-}10mm}$ plus $LN_{4\text{-}8mm}$). The light blue lines denote the neck node levels using the 2013 updated consensus guidelines. The color wash changes from blue through yellow to red indicate the probability increase. *Abbreviations:* $LN_{\geq 10mm}$ = cervical LNs meeting the diagnostic criteria for LN metastases; $LN_{\geq 8mm}$ = cervical LNs with a minimal axial diameter of ≥8 mm or any size with central necrosis, a contrast-enhanced rim, or extracapsular spread; $LN_{\geq 4mm}$ = cervical LNs with a minimal axial diameter ≥4 mm or any size with central necrosis, a contrast-enhanced rim, or extracapsular spread.

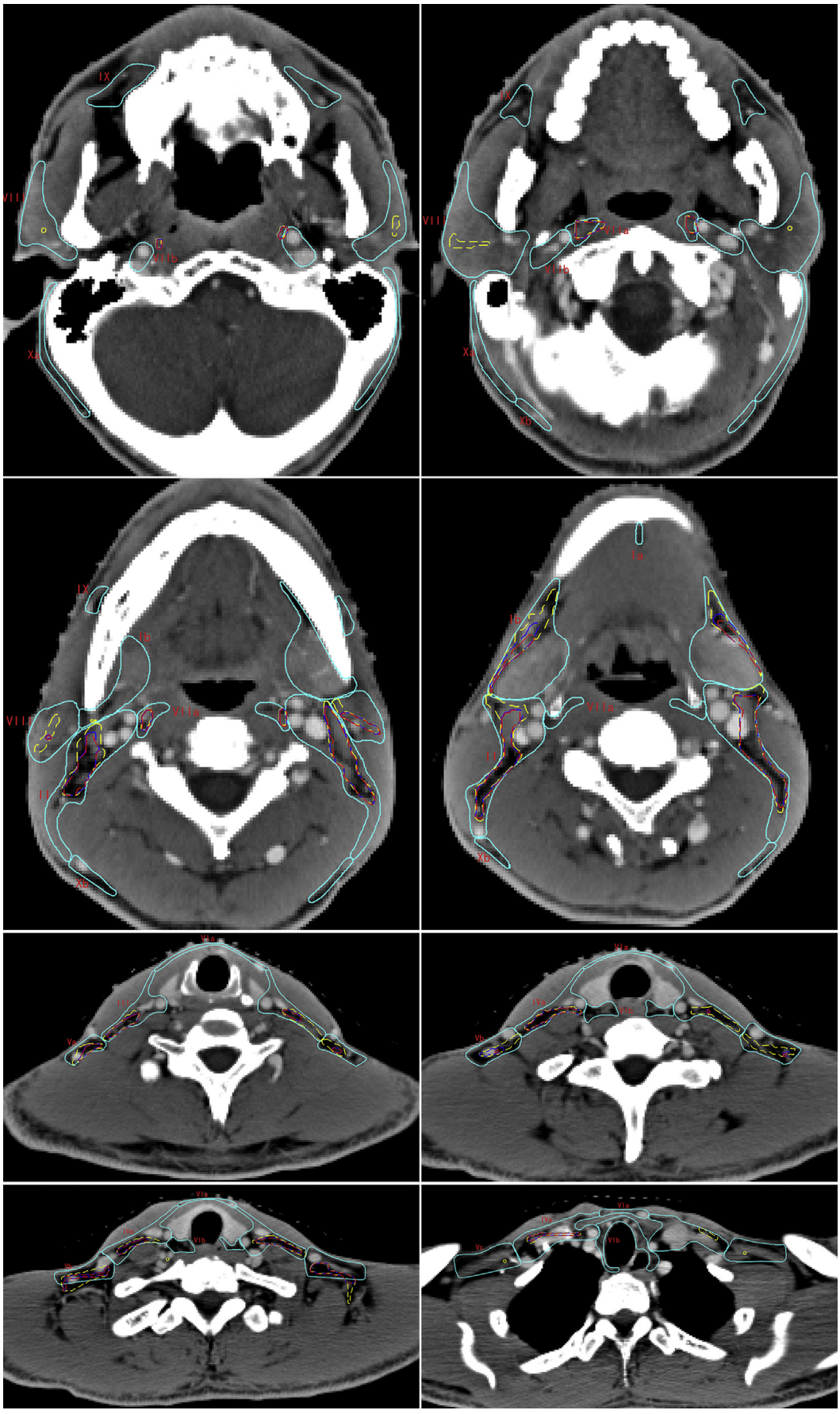
IX
VII
Ib
VIIa
VIIb
XI
XII
Ia
II
III
IVa
IVb
V
Va
Vb
VIa
VIb

radiologically negative LNs. Consequently, for more comprehensive consideration of potential risk areas to overcome the limitations of the absence of pathologic confirmation, we marked all LNs with a MID of ≥4 mm.

To the best of our knowledge, this is the first time that very extensive neck LN distribution probability maps were established for NPC, which visually demonstrate the distribution of neck LNs and can be used to guide the delineation of neck CTV boundaries, while previous studies were all based on image reading (14-18). Based on the distribution probability maps and distribution curves generated from LNs with a MID ≥4 mm, we have proposed a new level, level VIIc, to include the medial group of retropharyngeal LNs. Although only 5 cases (0.3%) had LNs located in the medial group, it cannot be denied that medial retropharyngeal LN is a part of the neck lymphatic drainage network of NPC. To minimize irradiation to constrictor muscles, we have proposed the caudal boundary of level VIIc should be set at the caudal edge of the C2 vertebrae. However, the proposed boundaries should be optimized in a larger patient cohort. Moreover, determining which cases require prophylactic irradiation of level VIIc warrants further investigation.

From our results, we suggest extending the posteromedial boundary of level Vb and the cranial boundary of level VIIa. For level Vb, we have confirmed that in 13.3% of cases (11 of 83), the neck LNs beyond the posteromedial border of level Vb are beyond that border, rather than resulting from differences in patient positioning (Fig. E5; available online at www.redjournal.org). Similarly, an insufficient posterior boundary was found previously by reviewing MRI scans from 3100 patients with NPC (14). Wang et al (15) suggested including the area between the levator scapulae and the anterior edge of the trapezius muscle as the CTV, similar to our suggestion. For level VIIa, Wang et al (15) assessed 597 retropharyngeal LNs in 392 patients and found 37 (6.2%) were at the level of the occipital bone, beyond the cranial border of the body of C1. Liu et al (16) reported that 24 retropharyngeal LNs (9.6%) were located at the occipital level. These previously reported data seem greater than our results (12 of 819; 1.5%). One reason could be that these studies assessed the entire volume of the enlarged LNs, but our probability maps and distribution curves included only the center point of the median slice of each LN to minimize the mass and distortion effects of enlarged LNs. Nevertheless, these previous results still support our modifications for level VIIa to some extent.

Owing to the impossibility of a complete pathologic examination of the lymphoid adipose tissue in NPC patients, our suggestions to reduce the boundaries of levels Ib, II, IVa, and Vc should be treated with caution because our LN distribution probability maps and distributions curves were simply image concerned, and whether they are consistence with true neck lymphatic drainage is unknown. Accordingly, our suggestions should not be adopted as routine clinical practice before an international consensus has been reached to reduce the LN level boundaries. Nevertheless, all our suggestions were based on the objective neck LN distribution from 959 patients and provide a foundation for further prospective studies and perhaps a revision of the guidelines.

For level Ib, it has been commonly accepted that elective irradiation should be considered in certain cases, such as gross involvement of the ipsilateral SMG, oral cavity, or anterior half of nasal cavity (17). After a comprehensive analysis of 1084 level Ib LNs with an MID of ≥4 mm from 959 patients, we have confirmed that no LN was identified along the medial edge of SMG or within the gland parenchyma. Therefore, we have suggested that the SMG might be spared when delineating the CTV of level Ib. Previously, Poon et al (6) reported a similar phenomenon in head and neck cancer and suggested that beyond the scenario of oral tongue cancer, the SMG parenchyma do not need to be included in a typical elective nodal target volume. Moreover, xerostomia is the most common side effect of radiation therapy for NPC, and preservation of SMG function is crucial to reduce the incidence of xerostomia, because the SMG produces most of the unstimulated saliva (7). However, for NPC, the safety of SMG sparing must be verified in prospective clinical trials.

For level II, the LN distribution we found showed that the gap between the sternocleidomastoid and splenius capitis muscles might be spared when delineating the CTV of level II where they are tightly integrated. This was similar to the recommendation by Zhang et al (18). Although Zhang et al (18) and Wang et al (19) reported the cranial edge of level II did not fully cover all level II involvement, it was not verified by our study, perhaps because we assessed only the LN center point rather than the total volume.

For levels IVa and Vc, although our study was simply image-concerned and no previous studies have focused on these 2 levels, reducing the boundaries would have potential benefits for NPC patients. For level IVa, modifying the

Fig. 3. Lymph node (LN) distribution curves (DCs) and the 2013 updated consensus guidelines demonstrated through 8 transverse sections. The light blue lines denote the neck LN levels using the latest international consensus guidelines. The red dotted lines denote the $DC_{\geq 10mm}$, generated using retropharyngeal LNs (LN_{RP}; ie, level VIIa) and $LN_{\geq 10mm}$; dark blue dotted lines denote $DC_{\geq 8mm}$, generated using on LN_{RP} and $LN_{\geq 8mm}$ ($LN_{\geq 10mm}$ plus $LN_{8\text{-}10mm}$); and yellow dotted lines denote $DC_{\geq 4mm}$, generated using LN_{RP} and $LN_{\geq 4mm}$ ($LN_{\geq 10mm}$ plus $LN_{8\text{-}10mm}$ plus $LN_{4\text{-}8mm}$). *Abbreviations:* $LN_{\geq 10mm}$ = cervical LNs meeting the diagnostic criteria for LN metastases; $LN_{\geq 8mm}$ = cervical LNs with a minimal axial diameter of ≥8 mm or any size with central necrosis, a contrast-enhanced rim, or extracapsular spread; $LN_{\geq 4mm}$ = cervical LNs with a minimal axial diameter ≥4 mm or any size with central necrosis, a contrast-enhanced rim, or extracapsular spread.

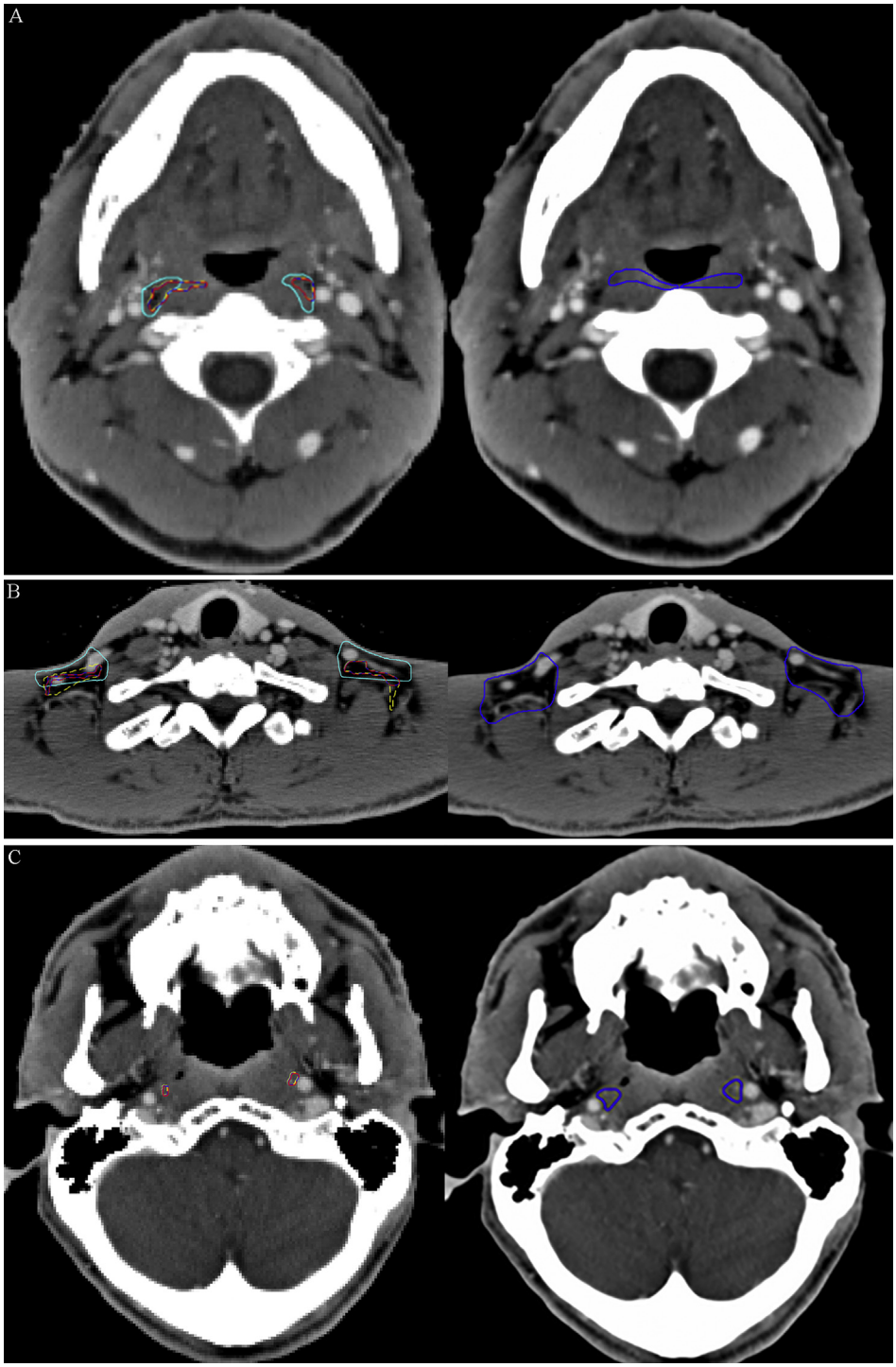

Fig. 4. Illustrations of proposed new level VIIc and modifications of neck lymph node (LN) level boundaries for level VIIa, Vb, Ib, II, IVa, and Vc. (Left) Three distribution curves (red dotted lines, dark blue dotted lines, and yellow dotted lines) and 2013 updated consensus guidelines (light blue lines). (Right) Proposed modifications: (A) A new level VIIc to include the medial group of retropharyngeal LN; (B) extension of the posteromedial border of level Vb to the anterior edge of the levator scapulae muscle to include the transverse blood vessels; (C) extension of the cranial border of level VIIa from the upper edge of C1 to the skull base; (D) sparing of the submandibular gland when delineating the clinical target volume (CTV) of level Ib; (E) sparing of gap between sternocleidomastoid and splenius capitis muscles when delineating the CTV of level II where they are tightly integrated; (F) modification of anterior border of level IVa from the anterior edge of the sternocleidomastoid to the posterior edge of the infrahyoid ribbon muscles; and (G) revision of anterior border of level Vc to the omohyoid muscle to replace the skin as the border.

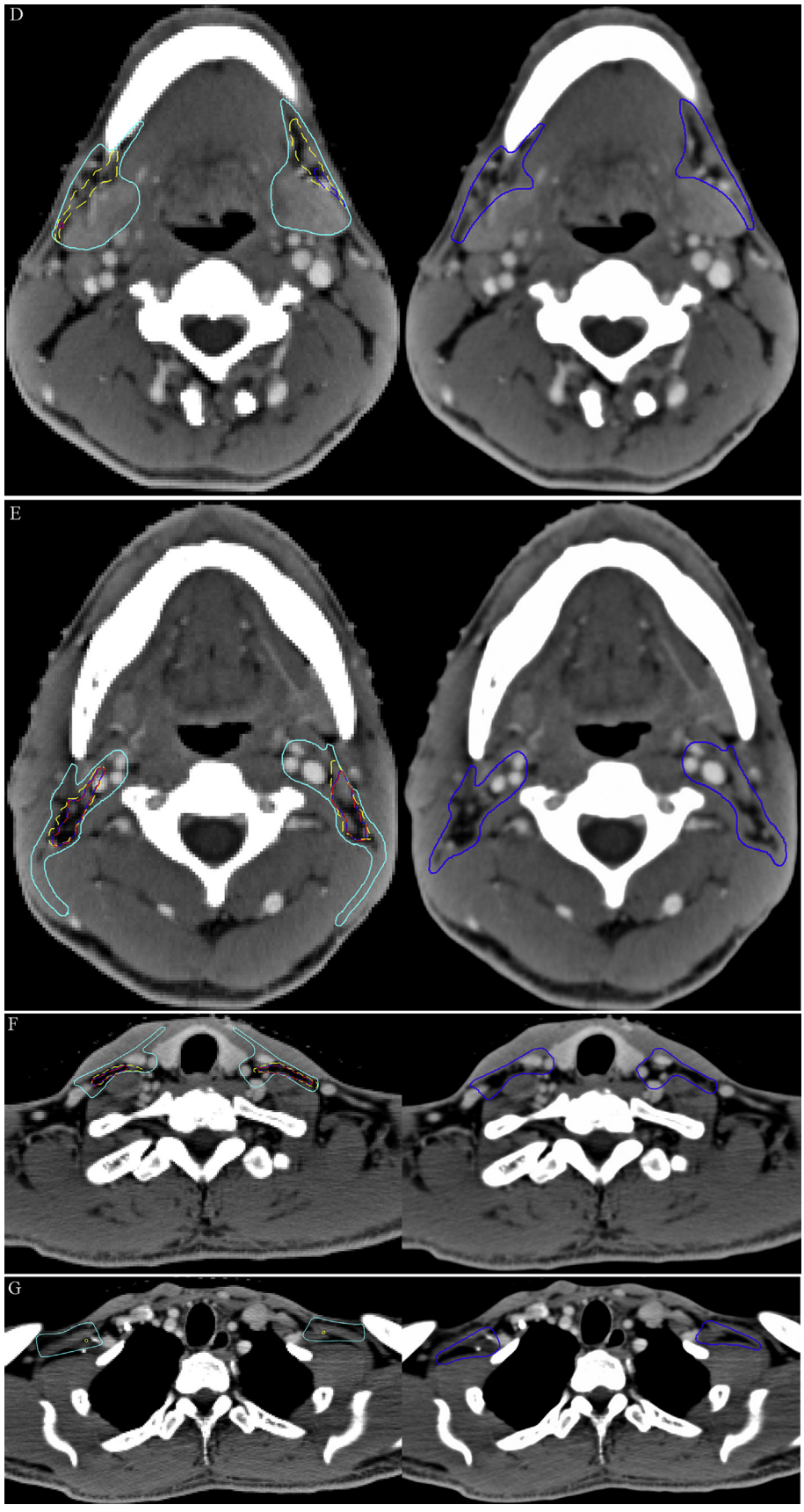

Fig. 4. *(Continued).*

anterior border to the posterior edge of the infrahyoid ribbon muscles could reduce the dose to the thyroid gland and might result in a decreased incidence of long-term hypothyroidism (20, 21). At level Vc, the superficial skin is right at the area of skin folds and is prone to friction and breakage. If the anterior boundary of level Vc was modified from the skin to the omohyoid muscle, the dose to the skin could be reduced and might eliminate radiation-induced dermatitis, one of the most common acute side effects of radiation and is dose dependent (22). Despite these potential benefits, our suggestions require further confirmation in larger patient cohorts and prospective studies.

Another issue to be addressed is that we marked the center point of each LN on all emerged slices, but used only the center point of the median slice to establish the distribution probability maps and distribution curves to minimize the mass and distortion effects of enlarged LNs. In the future, we will attempt to predict further LN metastasis probabilities of objective patients using this more comprehensive LN distribution information.

Conclusions

We established regional LN distribution probability maps and curves for NPC and confirmed that most LN levels in the 2013 updated consensus guidelines are comprehensive and applicable to NPC. However, we have proposed a new level, level VIIc, to include the medial group of retropharyngeal LNs, recommended moderately extended boundaries for levels Vb and VIIa, and suggested that the boundaries for levels Ib, II, IV, and Vc might be reduced.

References

1. Lee AW, Poon YF, Foo W, et al. Retrospective analysis of 5037 patients with nasopharyngeal carcinoma treated during 1976-1985: Overall survival and patterns of failure. *Int J Radiat Oncol Biol Phys* 1992;23:261-270.
2. Ho FC, Tham IW, Earnest A, et al. Patterns of regional lymph node metastasis of nasopharyngeal carcinoma: A meta-analysis of clinical evidence. *BMC Cancer* 2012;12:98.
3. Grégoire V, Levendag P, Ang KK, et al. CT-based delineation of lymph node levels and related CTVs in the node-negative neck: DAHANCA, EORTC, GORTEC, NCIC, RTOG consensus guidelines. *Radiother Oncol* 2003;69:227-236.
4. Gregoire V, Eisbruch A, Hamoir M, et al. Proposal for the delineation of the nodal CTV in the node-positive and the post-operative neck. *Radiother Oncol* 2006;79:15-20.
5. Gregoire V, Ang K, Budach W, et al. Delineation of the neck node levels for head and neck tumors: A 2013 update. DAHANCA, EORTC, HKNPCSG, NCIC CTG, NCRI, RTOG, TROG consensus guidelines. *Radiother Oncol* 2014;110:172-181.
6. Poon I, Fischbein N, Lee N, et al. A population-based atlas and clinical target volume for the head-and-neck lymph nodes. *Int J Radiat Oncol Biol Phys* 2004;59:1301-1311.
7. Hawkins PG, Lee JY, Mao Y, et al. Sparing all salivary glands with IMRT for head and neck cancer: Longitudinal study of patient-reported xerostomia and head-and-neck quality of life. *Radiother Oncol* 2017; https://doi.org/10.1016/j.radonc.2017.08.002.
8. Tang L, Mao Y, Liu L, et al. The volume to be irradiated during selective neck irradiation in nasopharyngeal carcinoma: Analysis of the spread patterns in lymph nodes by magnetic resonance imaging. *Cancer* 2009;115:680-688.
9. van den Brekel MW, Stel HV, Castelijns JA, et al. Cervical lymph node metastasis: Assessment of radiologic criteria. *Radiology* 1990; 177:379-384.
10. Friedman M, Mafee MF, Pacella BL Jr., et al. Rationale for elective neck dissection in 1990. *Laryngoscope* 1990;100:54-59.
11. Righi PD, Kopecky KK, Caldemeyer KS, et al. Comparison of ultrasound-fine needle aspiration and computed tomography in patients undergoing elective neck dissection. *Head Neck* 1997;19:604-610.
12. van den Brekel MW, Castelijns JA, Stel HV, et al. Modern imaging techniques and ultrasound-guided aspiration cytology for the assessment of neck node metastases: A prospective comparative study. *Eur Arch Otorhinolaryngol* 1993;250:11-17.
13. Vandecaveye V, De Keyzer F, Vander Poorten V, et al. Head and neck squamous cell carcinoma: Value of diffusion-weighted MR imaging for nodal staging. *Radiology* 2009;251:134-146.
14. Wang X, Hu C, Ying H, et al. Patterns of lymph node metastasis from nasopharyngeal carcinoma based on the 2013 updated consensus guidelines for neck node levels. *Radiother Oncol* 2015; 115:41-45.
15. Wang XS, Hu CS, Ying HM, et al. Patterns of retropharyngeal node metastasis in nasopharyngeal carcinoma. *Int J Radiat Oncol Biol Phys* 2009;73:194-201.
16. Liu LZ, Zhang GY, Xie CM, et al. Magnetic resonance imaging of retropharyngeal lymph node metastasis in nasopharyngeal carcinoma: Patterns of spread. *Int J Radiat Oncol Biol Phys* 2006;66: 721-730.
17. Zhang F, Cheng YK, Li WF, et al. Investigation of the feasibility of elective irradiation to neck level Ib using intensity-modulated radiotherapy for patients with nasopharyngeal carcinoma: A retrospective analysis. *BMC Cancer* 2015;15:709.
18. Zhang J, Pan L, Ren J, et al. Level IIb CTV delineation based on cervical fascia anatomy in nasopharyngeal cancer. *Radiother Oncol* 2015;115:46-49.
19. Wang X, Li L, Hu C, et al. Patterns of level II node metastasis in nasopharyngeal carcinoma. *Radiother Oncol* 2008;89:28-32.
20. Lee V, Chan SY, Choi CW, et al. Dosimetric predictors of hypothyroidism after radical intensity-modulated radiation therapy for non-metastatic nasopharyngeal carcinoma. *Clin Oncol* 2016;28:e52-e60.
21. Wu YH, Wang HM, Chen HH, et al. Hypothyroidism after radiotherapy for nasopharyngeal cancer patients. *Int J Radiat Oncol Biol Phys* 2010;76:1133-1139.
22. Salvo N, Barnes E, van Draanen J, et al. Prophylaxis and management of acute radiation-induced skin reactions: A systematic review of the literature. *Curr Oncol* 2010;17:94-112.